

1 **Lower crustal assimilation in oceanic arcs: insights**
2 **from an osmium isotopic study of the Lesser Antilles**

3 **Rachel Bezard^{1,2*}, Bruce F. Schaefer², Simon Turner², Jon P. Davidson¹ and David**
4 **Selby¹**

5 ¹ *Durham Geochemistry Centre, Department of Earth Sciences, Durham University,*
6 *South Road, Durham DH1 3LE, UK*

7 ² *Department of Earth and Planetary Sciences, Macquarie University, University*
8 *Avenue, Macquarie Park NSW 2113, Australia*

9 **Corresponding author. Now at Institut für Planetologie, Westfälische Wilhelms-*
10 *Universität Münster, Wilhelm-Klemm-Str. 10, 48149 Münster. Germany; E-mail address:*
11 *bezard@uni-muenster.de; Tel.: +49 251 83 33492; Fax: +49 251 83 36301.*

12

13 **Abstract**

14 We present whole rock $^{187}\text{Os}/^{188}\text{Os}$ data for the most mafic lavas along the Lesser
15 Antilles arc (MgO = 5-17 wt. %) and for the subducting basalt and sediments. $^{187}\text{Os}/^{188}\text{Os}$
16 ratios vary from 0.127-0.202 in the arc lavas. Inverse correlations between $^{187}\text{Os}/^{188}\text{Os}$
17 and Os concentrations and between $^{187}\text{Os}/^{188}\text{Os}$ and indices of differentiation such as
18 MgO suggests that assimilation, rather than source variation, is responsible for the range
19 of Os isotopic variation observed. $^{87}\text{Sr}/^{86}\text{Sr}$, La/Sm and Sr/Th are also modified by
20 assimilation since they all correlate with $^{187}\text{Os}/^{188}\text{Os}$. The assimilant is inferred to have a
21 MORB-like $^{87}\text{Sr}/^{86}\text{Sr}$ with high Sr (>700 ppm), low light on middle and heavy rare earth
22 elements (L/M-HREE; La/Sm ~2.5) and $^{187}\text{Os}/^{188}\text{Os} > 0.2$. Such compositional features
23 are likely to correspond to a plagioclase-rich early-arc cumulate. Given that assimilation
24 affects lavas that were last stored at more than 5 kbar, assimilation must occur in the
25 middle-lower crust.

26 Only a high MgO picrite from Grenada escaped obvious assimilation (MgO =
27 17% wt. %) and could reflect mantle source composition. It has a very radiogenic
28 $^{87}\text{Sr}/^{86}\text{Sr}$ (0.705) but a $^{187}\text{Os}/^{188}\text{Os}$ ratio that overlaps the mantle range (0.127).
29 $^{187}\text{Os}/^{188}\text{Os}$ and $^{87}\text{Sr}/^{88}\text{Sr}$ ratios of the sediments and an altered basalt from the subducting
30 slab vary from 0.18-3.52 and 0.708-0.714. We therefore suggest that, unlike Sr, no Os
31 from the slab was transferred to the parental magmas. Os may be either retained in the
32 mantle wedge or even returned to the deep mantle in the subducting slab.

33 **1. INTRODUCTION**

34 Understanding the behaviour of siderophile elements such as Os in subduction
35 zones is important for both scientific and economic reasons. Whether Os stays in the
36 subducting slab, is transferred to residual phases of the upper mantle, or is recycled back
37 to the crust via the magma needs to be constrained in order to (1) better estimate the
38 crust-mantle fluxes of siderophile elements throughout Earth evolution; (2) constrain
39 their application as a powerful isotope tracer to understand subduction processes; and (3)
40 understand the formation of precious metal ore-bodies.

41 In this context, the origin of radiogenic $^{187}\text{Os}/^{188}\text{Os}$ ratios within arc lavas,
42 compared to the depleted upper mantle (DMM), has been debated for more than a decade
43 (Borg et al., 2000; Alves et al., 2002; Chesley et al., 2002; Righter et al., 2002). While the
44 enrichment in radiogenic Os could be due to contamination of the mantle wedge by slab
45 derived fluids/melts (e.g. Borg et al., 2000; Alves et al., 2002), it could also be caused by
46 assimilation of arc crust during the magmatic ascent (Righter et al., 2002), or both
47 (Suzuki et al., 2011). Arguments for crustal assimilation include (1) a negative
48 correlation between $^{187}\text{Os}/^{188}\text{Os}$ and Os that is observed in most arcs lavas (Chesley et al.,
49 2002; Righter et al., 2002); (2) the very low Re concentrations in primitive arc lavas
50 coupled with the results of experimental studies predicting that slab derived-fluids
51 capable of carrying Os would carry several order of magnitude more Re than Os (Righter
52 et al., 2002; Xiong and Wood, 1999; 2000). Since both Re and Os were shown to be
53 similarly volatile (Finnegan et al., 1990), the absence of high Re concentrations in
54 primitive lavas suggests that Re from the slab is not efficiently transported into primitive
55 magmas, in which case Os is very unlikely to be transported too; and (3) the very

56 unradiogenic $^{187}\text{Os}/^{188}\text{Os}$ of some mantle xenoliths from the Japan and Izu Bonin arcs
57 (Parkinson et al., 1998; Senda et al., 2007) which suggest the absence of enrichment in
58 radiogenic Os of the mantle wedge. On the other hand, a slab origin for radiogenic Os in
59 arc lavas is supported by (1) the radiogenic signature of some mantle xenoliths from the
60 Cascades, Japan, New Ireland and Kamchatka arcs (Brandon et al., 1996; McInnes et al.,
61 1999; Widom et al., 2003); (2) the trend to more radiogenic $^{187}\text{Os}/^{188}\text{Os}$ with decreasing
62 Cr# and increasing Fe^{3+} in Cr-spinels from the Izu Bonin arc which suggests an increase
63 in mobility of slab derived Os during an arc lifetime due to a progressive change in
64 oxidation state of the mantle (Suzuki et al., 2011); and (3) the existence, in high-pressure
65 melange zones, of ‘hybrid’ rocks between crustal and mantle materials which display
66 similar inverse correlation between Os and $^{187}\text{Os}/^{188}\text{Os}$ to that observed in most arc lavas
67 (Penniston-Dorland et al., 2012; 2014)

68 The Lesser Antilles arc (Fig. 1) is an excellent natural laboratory to investigate the
69 mobility of Os in subduction zones since: (1) very primitive lavas such as picrites with
70 $\text{MgO} = 17.4$ (wt. %) can be sampled; (2) very radiogenic Os should be subducted in the
71 southern part of the subduction zone where the slab contains organic-rich sediments
72 (black shales); and (3) the arc lavas and the subducting slab sediment/basalts are both
73 very well constrained in terms of major, trace elements and radiogenic isotopes.
74 Accordingly, we have analysed the most mafic and well constrained lavas from along the
75 arc, as well as representative sediments and altered basalt from the subducting slab.

76

77 **2. SAMPLES AND ANALYTICAL METHODS**

78 **2.1 Samples**

79 We selected the most mafic lava samples (MgO=5-17 wt. %) available from 7
80 different islands along the Lesser Antilles arc (n=8), as well as an altered basalt (n=1;
81 DSDP site 543), an organic-poor sediment (n=1; DSDP site 543) and organic-rich
82 sediments including black shales (n=11; Unit 3-5 DSDP site 144) from the subducting
83 American Plate (Tables 1 and 2).

84 The sediments were selected to characterize a key north-south difference in the
85 nature of the subducting sediments, likely to be reflected in their Os isotopic signature.
86 The nature and composition of the sediments present at the front of the arc was
87 investigated by Hayes et al. (1972), Pudsey and Reading (1982) and Biju-Duval et al.
88 (1984; 1985) using cored sediments from the DSDP site 543 for the northern sequences
89 and DSDP site 144 and Barbados sediments for the southern sequences. These studies
90 showed that the northern subducting pile (north of Martinique) was dominated by clays
91 and radiolarites while the southern subducting pile (Martinique and southward) was
92 mainly composed of clay and carbonate with the occurrence of significant amounts of
93 organics (up to 30%), biogenic silica (up to 30%) and detrital quartz (up to 40%) in some
94 units. In terms of Os isotopes, the most important difference between the northern and the
95 southern sequences is the presence of (Late Cretaceous) organic-rich layers at the base of
96 the southern sedimentary pile (the absence of such organic-rich units in the north is due
97 to the younger age of the subducting plate, as supported by the magnetic map of the
98 Atlantic Ocean floor at the front of the arc). This is because organic-rich sediments
99 typically concentrate Re during deposition and are expected to present higher $^{187}\text{Os}/^{188}\text{Os}$
100 than organic-poor sediments, due to Re decay. The presence of more radiogenic Os in the
101 southern subducting pile could in turn be reflected in the lava compositions. Therefore,

102 analysing both organic-rich and organic-poor sediments is important to understand if, as
103 predicted, they have different isotopic composition.

104 The organic-poor sediment analysed consists of early Miocene clay with minor
105 ash (Biju-Duval et al., 1984). The organic-bearing sediments selected record
106 sedimentation preceding (Unit-5-4; up to 5% organics; Late-Aptian to lower
107 Cenomanian; Carpentier et al., 2008) and contemporaneous (Unit-3; up to 30% organics;
108 Lower Turonian to Santonian) with the oceanic anoxic event 2 (OAE2; 93.5 My e.g.
109 Turgeon and Creaser, 2008). Samples from Unit 5 consist of quartzose carbonaceous clay
110 or mudstone while Unit 4 sample is marl. Finally samples from Unit 3 are zeolitic
111 calcareous carbonaceous black shale (Hayes et al., 1972).

112 By selecting the most mafic lavas, we attempted to minimise the effects of
113 assimilation of continent-derived sediment present in the arc crust. Such sediment is
114 responsible for the extreme isotopic compositions observed in the central-southern parts
115 of the arc (e.g. Davidson, 1987; Bezard et al., 2014). All lavas (Fig. 2) and sediments
116 have previously been analysed for major, trace elements and Sr-Nd isotopes (Davidson,
117 1984; Davidson, 1986; Heat et al., 1998; Van Soest, 2000; Dufrane et al., 2009; see Table
118 2). The most primitive lava sampled, which is also the most primitive lava in the arc, is
119 an olivine and plagioclase phyric picrite from Grenada (LAG4) with both high MgO
120 (17.4 wt. %) and Mg# (77.4) (Van Soest, 2000). It belongs to the abundant M-series suite
121 of picrites found on the island. Previous studies on M-series picrites with MgO as high as
122 15.5 wt. % suggested that these were primary mantle melts by precluding olivine
123 phenocrysts accumulation, or incorporation of mantle xenocrysts, as the cause of their
124 high MgO. LAG 4 olivine crystals have similar Mg# in cores (90-82) and rims (89-82)

125 which does not support a xenocrystic origin of the crystals. Furthermore, the D_{Ni}
126 calculated from the picrite MgO ($D_{Ni} = 6.27$; using Hart and Davis (1978) equation) is
127 similar to the D_{Ni} calculated using the whole rock and the mean olivine Ni concentrations
128 ($D_{Ni} = 6.67$; using probe data from Van Soest (2000)). This suggest that the Ni content in
129 the olivine crystals is consistent with that expected from crystals growing in a magma
130 with an MgO similar to that of LAG4 and that no significant olivine accumulation or
131 mantle xenocryst incorporation should have occurred. Out of the samples selected, it
132 displays the highest Light on Middle Rare Earth Element ratio (L/M-HREE), the lowest
133 Sr/Th and the most radiogenic Sr isotopic composition (Sr/Th = 123; $^{87}Sr/^{86}Sr = 0.7051$;
134 Fig. 2). Such features characterise all Grenada primitive lavas when compared to basaltic
135 lavas from other islands of the arc (Macdonald et al., 2000). St Vincent contains very
136 mafic lavas (MgO = 12.6 wt. %) with phenocryst assemblages dominated by olivine
137 (traces of Cpx and Ti-magnetite). A less primitive basalt from the same island (MgO =
138 5.12 wt. %) mainly presenting plagioclase, olivine and clinopyroxene phenocrysts was
139 also analysed. The most primitive lavas from the remaining islands (Saba, Redonda,
140 Guadeloupe, Martinique and St Lucia) have MgO contents that range from 5.1 to 8.7 (wt.
141 %). Their phenocryst assemblage comprise olivine crystals and variable amount of
142 clinopyroxene and plagioclase. All of the lavas selected are 1 Ma old or younger with the
143 exception of the St Lucia lava flow which is dated at 11 Ma (Table 1).

144 **2.2. Analytical methods**

145 All samples, except the organic-rich sediments, were analysed for Os and
146 $^{187}Os/^{188}Os$ at the Geochemical Analysis Unit (GAU) at Macquarie University. The
147 organic-rich sediments were analysed for Re, Os and isotope compositions ($^{187}Re/^{188}Os$;

148 $^{187}\text{Os}/^{188}\text{Os}$) at the TOTAL Laboratory for Source Rock Geochronology and
149 Geochemistry which is part of the Durham Geochemistry Centre (DGC) at Durham
150 University.

151 At Macquarie, whole rock powders (2-5g) (produced in agate ball mills) were
152 spiked for Os and digested using large carius tubes (60 cm³) in inverse *aqua-regia* using
153 double Teflon distilled reagents at 220°C for 3 days. Given the young age of the samples,
154 no age correction on the $^{187}\text{Os}/^{188}\text{Os}$ ratio was necessary and Re was not analysed. Os was
155 separated by solvent extraction following the method of Cohen and Waters (1996) and
156 was analysed by negative thermal ion mass spectrometry (N-TIMS) on the electron
157 multiplier (SEM) of the Thermo-Finnigan Triton mass spectrometer at Macquarie
158 University in dynamic mode. All data were blank corrected using the total procedural
159 blank (TPB) processed with the samples analysed. TPB was 6.30 pg Os with an
160 $^{187}\text{Os}/^{188}\text{Os}$ ratio of 0.1821 (n=1). This corresponds to corrections of 0-12% except for the
161 two lavas with the lowest abundances where these corrections amounted to 21 and 25%.
162 During the analytical session, instrument performance was monitored by analysis of Os
163 in-house solution standard JMC-2. $^{187}\text{Os}/^{188}\text{Os}$ for 5 ng loads in dynamic collection mode
164 was 0.18311 ± 0.00016 (2SD; n=4) which is in good agreement with the long term
165 running means of 5ng JMC-2 in dynamic mode of 0.18294 ± 0.00070 (2SD; n=17 since
166 2006). The performance of the instrument when running small loads similar to the lavas
167 was verified by the analysis of ~1.7ng loads of WPR-1 (0.1g digested). The average
168 $^{187}\text{Os}/^{188}\text{Os}$ ratio of the WPR-1 international rock standard was 0.1451 ± 0.0013 (2SD;
169 n=4) with concentrations of $17.19 \text{ ppb} \pm 0.71$ (2SD; n=4) which is in good agreement

170 with the accepted values (Cohen and Waters, 1996; $^{187}\text{Os}/^{188}\text{Os} = 0.14543 \pm 0.00018$
171 (2SD) and $\text{Os} = 16.06 \text{ ppb} \pm 0.8$ (2SD)).

172 At Durham, the organic-rich whole rock powders were also analysed by isotope-
173 dilution negative thermal ionization mass spectrometry. Prior to being powdered, all the
174 samples were cleaned to remove any minor drill marks using a diamond polish cloth with
175 no polishing agent, except water. Samples were pre crushed without metal contact and
176 then powdered in a Zr dish. A dried sample weight of $\geq 30 \text{ g}$ was powdered in order to
177 homogenise the Re and Os within the sample (Kendall et al., 2009). The Re-Os isotopic
178 analysis was conducted using Carius tube digestion in a 0.25 g/g CrO_3 4N H_2SO_4 reagent
179 at 220°C for 48hrs with the Re and Os isolated from the acid medium using solvent
180 extraction, micro-distillation and anion chromatography methodology (Selby and
181 Creaser, 2003). This method preferentially liberates hydrogenous Re-Os (Selby and
182 Creaser, 2003; Kendall et al. 2009 and references therein). In brief, $\sim 0.5 \text{ g}$ of sample
183 powder was loaded in a Carius tube with a known amount of mixed tracer solution. ^{190}Os
184 + ^{185}Re , with 8 ml of CrO_3 - H_2SO_4 solution. The sealed Carius tubes were then placed in
185 an oven at 220°C for 48 hrs. Osmium was isolated and purified using solvent extraction
186 (CHCl_3) and microdistillation methods. Anion chromatography was used to purify the Re
187 from 1 ml of the CrO_3 - H_2SO_4 solution (Selby and Creaser, 2003). The purified Re and Os
188 fractions were loaded onto Ni and Pt filaments, respectively (Selby and Creaser, 2003)
189 with the addition of $\sim 0.5 \mu\text{l}$ BaNO_3 and BaOH activator solutions, respectively. Isotope
190 compositions were measured using N-TIMS (Creaser et al., 1991; Volkening et al., 1991)
191 via faraday cups for Re and electron multiplier in peak hopping mode for Os. All samples
192 were analysed as one batch. For this batch the total procedural blank for Re and Os

193 during this study is 13.3 ± 1.8 pg and 0.32 ± 0.17 pg, respectively, with $^{187}\text{Os}/^{188}\text{Os}$ value
194 of 0.19 ± 0.05 . Uncertainties for $^{187}\text{Re}/^{188}\text{Os}$ and $^{187}\text{Os}/^{188}\text{Os}$ are determined through full
195 propagation of uncertainties in Re and Os mass spectrometer measurements, blank
196 abundances and isotopic compositions, spike calibrations and reproducibility of standard
197 Re and Os isotopic values. In-house standard solutions (DROsS and Re Std) are 0.16094
198 ± 0.00030 and 0.5980 ± 0.0032 (2 S.D.), which are consistent within uncertainty to those
199 published by Nowell et al. (2008). Additionally at Durham, sample Re-Os data
200 reproducibility is monitored using the USGS rock reference material SDO-1 (Devonian
201 Ohio Shale). Average (2 S.D.) Re-Os data for SDO-1 are: 75.5 ppb ± 11.3 Re, and 626.1
202 ppt ± 101.8 Os, and 1166.0 ± 88.1 $^{187}\text{Re}/^{188}\text{Os}$ and 7.831 ± 0.568 $^{187}\text{Os}/^{188}\text{Os}$ (Du Vivier
203 et al., 2014).

204 3. RESULTS

205 All $^{187}\text{Os}/^{188}\text{Os}$ and Os concentrations as well as $^{187}\text{Re}/^{188}\text{Os}$ and Re for the
206 organic-rich sediments are presented in Table 1 and corresponding lithophile element
207 concentrations and isotopic ratios from the literature are presented in Table 2. All lavas
208 apart from the most mafic sample, (Grenada picrite; MgO = 17 wt. %), have more
209 radiogenic $^{187}\text{Os}/^{188}\text{Os}$ than the depleted mantle range (DMM; $^{187}\text{Os}/^{188}\text{Os} = 0.1238 \pm$
210 0.0042 ; Rudnick and Walker (2009)) and variable $^{187}\text{Os}/^{188}\text{Os}$ ratios and Os
211 concentrations ranging between 0.127-0.202 and 0.005-0.362 ppb respectively (Fig. 3).
212 The $^{187}\text{Os}/^{188}\text{Os}$ ratio of the altered basalt is 0.466 and this sample has a very low Os
213 abundance (0.0095 ppb). The organic-poor claystone from DSDP site 543 is enriched in
214 Os (11.15 ppb) and possesses moderately radiogenic $^{187}\text{Os}/^{188}\text{Os}$ (0.185). The most
215 organic-rich sedimentary units from DSDP 144 (Unit 3) have highly radiogenic

216 $^{187}\text{Os}/^{188}\text{Os}$ (1.33-3.25) and moderate Os concentrations (0.10-0.94 ppb), while the older
217 units (4 and 5), which are characterized by lower organic matter content, have moderately
218 radiogenic $^{187}\text{Os}/^{188}\text{Os}$ (0.32-0.72) and variable Os concentrations from 0.09 to 34.48
219 ppb. (Fig. 3). The abundances of Os in all sediments analysed is above that of average
220 continental crust (<50 ppt; Peuker-Ehrenbrink and Ravizza, 2000). The isotopic
221 variations observed between Unit 3 and Units 4 and 5 are also observed in the calculated
222 initial $^{187}\text{Os}/^{188}\text{Os}$ ratio (using sediment ages from Hayes et al. (1972) and Carpentier et
223 al. (2008); Table 1) which indicates that part of the isotopic variations observed in site
224 144 sediment are not due to variations in Re content. Given that the analytical method
225 used for these sedimentary units preferentially liberates hydrogenous Re and Os and not
226 detrital associated Re-Os, the variations of the initial isotopic ratios need to be inherited
227 from sea water compositional variations during sediment deposition.

228 **4. DISCUSSION**

229 **4.1 Crustal assimilation control on $^{187}\text{Os}/^{188}\text{Os}$**

230 In the Lesser Antilles arc, all studies addressing the quantification of the
231 subducting slab derived components in the magma source, using the isotopic (Sr, Nd, Pb,
232 Hf, U-series) and trace element composition of the lavas, suggested either a similar (e.g.
233 Davidson and Wilson (2011); Dufrane et al. (2009)) or increasing amount of sediment in
234 the mantle source along the arc (e.g. Carpentier et al., 2008). Therefore, if transfer of
235 slab-derived Os into the mantle wedge was to be reflected in the isotopic variations
236 observed in the lavas, a north-south trend to more radiogenic $^{187}\text{Os}/^{188}\text{Os}$ in the lavas
237 should be observed. This is because the dominantly organic-poor sediment sequences

238 subducted in the north have markedly less radiogenic $^{187}\text{Os}/^{188}\text{Os}$ than the sequences
239 subducted in the south which comprise organic-rich sediments. However, no such
240 geographic variation is observed. Indeed the least radiogenic compositions are observed
241 in lavas from the south of the arc, in Grenada and St Vincent. These observations argue
242 against the direct control of lava isotopic variations by slab-derived Os. Instead, the
243 samples form inverse correlations between $^{187}\text{Os}/^{188}\text{Os}$ and both Os (0.005-0.36) (Fig. 4a)
244 and MgO (Fig. 4b) with compositions of the southern lavas plotting on a steeper trend
245 than the northern islands (from Martinique northward). These negative correlations
246 between an index of differentiation and $^{187}\text{Os}/^{188}\text{Os}$ cannot easily be produced in the
247 mantle source since it would either need to be explained by (1) a mantle source with
248 homogeneous MgO, affected by a process able to enrich it in ^{187}Os and additionally
249 control the future extent of magmatic differentiation; or (2) a heterogeneous source
250 characterized by coupled variations in MgO and $^{187}\text{Os}/^{188}\text{Os}$ (e.g. in sources with a
251 different mineralogy due to metasomatism, such as a peridotitic mantle comprising
252 pyroxenites) that would be transmitted to the magma and conserved until eruption. Both
253 scenarios seem very unlikely since the degree of lava differentiation is known to be
254 influenced by the structure and thickness of the crust, both thought to be heterogeneous
255 along the arc (e.g. Boynton et al., 1979). Therefore, the $^{187}\text{Os}/^{188}\text{Os}$ variations in the
256 Lesser Antilles arc lavas is more likely accounted for by a process, or processes, which
257 postdate mantle melting. Since both trends formed by lavas from the southern and
258 northern islands back project toward the composition of the Grenada picrite (Fig. 4), they
259 could be explained by evolution from a common parental magma. The differences in
260 subsequent magmatic evolution may reflect either different phases fractionated during

261 assimilation with different partitioning for MgO and Os, different rates of assimilation or
262 slightly different $^{187}\text{Os}/^{188}\text{Os}$ ratios of the putative assimilants.

263 Control of the osmium isotopic composition by assimilation rather than by slab
264 contributions is emphasized when the $^{187}\text{Os}/^{188}\text{Os}$ ratios of both lavas and sediments are
265 plotted against Sr isotope ratios (Fig. 5a). Once again, a negative correlation is observed
266 for the lavas with a decrease in $^{87}\text{Sr}/^{86}\text{Sr}$ with increasing $^{187}\text{Os}/^{188}\text{Os}$. This negative
267 correlation precludes the simple mixing of sediment-derived Os in the lavas sources since
268 the sediments display both radiogenic Sr and Os and a mixing line between the mantle
269 and the sediments would therefore have a positive slope which is the opposite of that
270 observed (Fig. 5a). Although the altered basalt from the slab has a lower Sr isotopic
271 composition than the sediment, mixing of fluids derived from this component with the
272 mantle wedge would also result in a positive trend.

273 A source process capable of increasing slab-derived Os while decreasing slab
274 derived Sr in the mantle is inconsistent with the decrease in Os concentrations observed
275 with increasing $^{187}\text{Os}/^{188}\text{Os}$ (Fig. 4a). So too, stabilisation of an Os-bearing phase in the
276 mantle wedge due to fluid fluxing from the slab (Borg et al., 2000) is inconsistent with
277 the covariant decrease in both MgO and Os (Fig. 4a,b).

278 An increase in slab derived Os mobility in response to increasing the oxidation
279 state of the mantle through time (Suzuki et al., 2011) is inconsistent with the decrease in
280 $^{87}\text{Sr}/^{86}\text{Sr}$ observed with the increasing $^{187}\text{Os}/^{188}\text{Os}$ (Fig. 5a). Indeed slab derived Sr
281 mobility is very unlikely to be sensitive to variation in oxygen fugacity given that, unlike
282 Os, Sr displays only one valence state (bivalent) under normal geological conditions.

283 Instead, the contents of slab-derived Sr in the mantle are likely to be controlled by the
284 extent of slab-derived fluid fluxing through the wedge, the latter fluid being also
285 responsible for the increase in mantle oxygen fugacity through time (Brandon and
286 Draper, 1996). Therefore, an increase rather than a decrease in slab derived Sr with
287 increasing mantle oxygen fugacity would be expected. For example, such positive
288 correlation between Sr concentration and oxygen fugacity was observed in melt
289 inclusions from primitive lavas in the Cascades (Rowe et al., 2009). Furthermore,
290 because the increase in $^{187}\text{Os}/^{188}\text{Os}$ ratios correlates inversely with MgO, any postulated
291 increase in oxygen fugacity of the mantle would need to have a tight control on the future
292 degree of differentiation of the magma, which seems very unlikely.

293 Finally, a complex case occurring at the slab-mantle interface and involving (1) a
294 mechanical mixing of ultramafic and mafic material from the subducting slab around
295 blocks of subducted basalts and (2) the metasomatism of the resulting hybrid rocks by
296 sediment-derived fluids, was shown to produce a suite of rocks with similar negative
297 correlation between Os, MgO and $^{187}\text{Os}/^{188}\text{Os}$ to that observed in the Lesser Antilles
298 lavas (Penniston-Dorland et al., 2012; 2014). A negative correlation between $^{87}\text{Sr}/^{86}\text{Sr}$
299 and $^{187}\text{Os}/^{188}\text{Os}$ in these hybrid rocks would also be predicted. It has been suggested that,
300 if these rocks from the slab-mantle interface ascended within diapirs to the base of the arc
301 lithosphere (e.f. Marschall and Schumacher, 2012), these heterogeneities could be
302 directly reflected in the arc lavas (Penniston-Dorland et al., 2012; 2014). However, as
303 mentioned in the previous section, if the correlation observed in the lava compositions
304 resulted from a direct reflection of these source heterogeneities, then no, or similar
305 amounts of differentiation would need to have occurred for all lavas analysed, which

306 seems unlikely. Furthermore, rocks in the melange having $^{187}\text{Os}/^{186}\text{Os}$ out of the mantle
307 range are dominantly made of altered basalt and should therefore have high $\delta^{18}\text{O}$
308 signatures which would be transferred to the related magma. This scenario is inconsistent
309 with the mantle like $\delta^{18}\text{O}$ of the olivine and pyroxene crystals analysed in the Lesser
310 Antilles lavas with the highest $^{187}\text{Os}/^{188}\text{Os}$ ratios. Therefore, although source
311 contamination cannot be completely ruled out, it is considered highly unlikely, and the
312 trends defined by the lavas seem more plausibly explained by a process occurring after
313 melting in the source, .i.e. crustal assimilation.

314 **4.2 Source $^{187}\text{Os}/^{188}\text{Os}$**

315 Since crustal assimilation appears to have affected lava $^{187}\text{Os}/^{188}\text{Os}$ during
316 differentiation in the Lesser Antilles, the only sample suitable for constraining source
317 characteristics is the sample with the highest MgO and highest Os concentrations, which
318 is the picrite from Grenada (LAG4). This picrite $^{187}\text{Os}/^{188}\text{Os}$ (0.1267) plots within the
319 mantle range ($\text{DMM} = 0.1238 \pm 0.0042$) (Fig. 4a, b) which indicates that assimilation had
320 no, or very limited (in the case where the ambient mantle lies in the lower hand of the
321 DMM range), effect on its composition and that it therefore represent the lava with the
322 closest composition to that of the mantle source region. The apparent absence, or very
323 limited amount, of radiogenic Os from either the subducting altered basalt or sediments in
324 the Grenada picrite indicates either that (1) Os from the subducting slab is not, or not
325 efficiently, transported into the magma source regions or (2) that it was retained in a
326 residual mantle phase before the primitive Grenada melts were generated.

327 Conversely, the Grenada picrite has very radiogenic $^{87}\text{Sr}/^{88}\text{Sr}$ (0.70508; Fig 5a)
328 which indicates that, as expected, Sr was mobilised from the slab into the wedge. As

329 mentioned earlier, the more radiogenic Sr isotopic ratio of the Grenada picrite analysed,
330 compared to other islands of the arc, is a general feature of Grenada mafic lavas, which
331 has often been interpreted to reflect a greater contribution of sediment to the mantle
332 source (Thirlwall et al., 1996). However, we show that Sr isotopes correlate inversely
333 with Os isotopes which appear to be controlled by assimilation. Therefore, the negative
334 trend in $^{87}\text{Sr}/^{86}\text{Sr}$ observed in the Lesser Antilles lavas would need to be accounted for by
335 the same process. Hence $^{87}\text{Sr}/^{88}\text{Sr}$ in the Grenada picrite may not be more radiogenic than
336 primary magmas of the other islands along the arc but instead provide the only true
337 representative indication of source $^{87}\text{Sr}/^{86}\text{Sr}$ prior to crustal assimilation. In this case,
338 estimations of slab contributions to the magma source based on Sr isotopes in mafic lavas
339 would have historically been misestimated for most islands.

340 **4.3 Characteristics and nature of the assimilant**

341 *4.3.1 Trace element and isotopic characteristics*

342 As described in section 4.1, the lavas show an inverse correlation between
343 $^{87}\text{Sr}/^{86}\text{Sr}$ and $^{187}\text{Os}/^{188}\text{Os}$ (Fig. 5a). However, unlike MgO and Os vs. $^{187}\text{Os}/^{188}\text{Os}$, where
344 two trends are observed, no north-south separation of the data exists. Given that isotopic
345 ratios are not affected by crystal fractionation, we suggest that the same assimilant is
346 present in both the north and the south of the arc and that the north-south trends observed
347 on plots of MgO and Os vs. $^{187}\text{Os}/^{188}\text{Os}$ can be accounted for by different fractionated
348 assemblages during assimilation (i.e. different bulk partition coefficients). For example,
349 fractionation of olivine during assimilation will produce a steeper decrease in MgO and
350 Os compared with clinopyroxene fractionation.

351 Given that $^{87}\text{Sr}/^{86}\text{Sr}$ decreases down to ~ 0.703 , the assimilant must have $^{87}\text{Sr}/^{86}\text{Sr}$
352 close to the DMM (Salters and Stracke, 2004), which precludes any sedimentary origin
353 and is in agreement with the mantle-like clinopyroxene and olivine $\delta^{18}\text{O}$ data available
354 for some of the high $^{187}\text{Os}/^{188}\text{Os}$ lavas, which are similar to those of Grenada picrites
355 (Saba: $\delta^{18}\text{O}_{\text{ol}} = 5.13$ and $\delta^{18}\text{O}_{\text{cpx}} = 5.74$ for LAS1; Guadeloupe: $\delta^{18}\text{O}_{\text{ol}} = 5.00\text{-}5.12$ and
356 $\delta^{18}\text{O}_{\text{cpx}} = 5.51$ for GUAD510; Grenada: $\delta^{18}\text{O}_{\text{ol}} = 5.18$ for LAG4; Van Soest et al., 2002).
357 No clear correlation between Pb isotopes and $^{187}\text{Os}/^{188}\text{Os}$ can be observed and no
358 correlation between $^{143}\text{Nd}/^{144}\text{Nd}$ and $^{187}\text{Os}/^{188}\text{Os}$ exist (not shown). This could either
359 indicate that the isotopic composition of the assimilant is similar to that of the primitive
360 magma, or that the concentrations in Pb and Nd in the assimilant are not high enough to
361 buffer existing source variations between islands.

362 When La/Sm or La/Yb are plotted against $^{187}\text{Os}/^{188}\text{Os}$ (Fig. 5b), the same negative
363 correlation observed on plots of MgO and Os vs. $^{187}\text{Os}/^{188}\text{Os}$ exists. Such correlations
364 suggest that the REE were affected during assimilation. As with MgO and Os, we
365 propose that the separation of the samples into two similar trends is due to different
366 phases being fractionated during assimilation. The decrease in L/M-HREE in itself
367 (observed in both trends) could therefore reflect the interplay of the progressive
368 incorporation of a low La/Sm assimilant and of fractional crystallization of minerals that
369 fractionate L/M-HREE (such as clinopyroxene or amphibole).

370 Finally, Sr/Th seems also affected by crustal assimilation since it correlates
371 negatively with $^{187}\text{Os}/^{188}\text{Os}$ (Fig. 5c). The correlation is clearly due to increasing Sr since
372 Th does not decrease with $^{187}\text{Os}/^{188}\text{Os}$. As for $^{87}\text{Sr}/^{88}\text{Sr}$ vs. $^{187}\text{Os}/^{188}\text{Os}$, no distinction
373 between the north-south sections of the arc can be observed, consistent with a common

374 assimilant composition along the arc. The assimilant must also have very high Sr content
375 with a minimum Sr/Th of 624 (the highest ratio found in the lavas).

376 In summary, the isotopic and trace element composition of the lavas suggest that
377 one of the assimilants present in the basement of Lesser Antilles islands (the other being
378 continent-derived sediment, not discussed here) displays a mantle-like $^{87}\text{Sr}/^{88}\text{Sr}$ ratio, a
379 $^{187}\text{Os}/^{188}\text{Os}$ higher than 0.2, a high Sr/Th (> 620), and a low La/Sm and La/Yb.
380 Significantly, thermobarometric estimations performed on St Vincent picrite (STV301)
381 indicate that it was last stored at depths corresponding to the arc middle-lower crust (Heat
382 et al., 1998; Pichavant et al., 2007). This would imply that assimilation would need to
383 have occurred at depths equivalent to or greater than these.

384 *4.3.2 Nature of the assimilant*

385 Recent (\sim late Cretaceous to Paleogene) altered Mid-Ocean Ridge Basalts
386 (MORB) or Fore-arc Basalts (FAB; Reagan et al. (2010)) could have a DMM-like
387 $^{87}\text{Sr}/^{86}\text{Sr}$ with $^{187}\text{Os}/^{188}\text{Os}$ higher than 0.2 and low L/M-HREE (typically <1), but their Sr
388 concentration is typically far too low (typically ≤ 90 ppm) to be able to modify the
389 primitive magma concentrations. Bulk mafic MORB or FAB cumulates would also be
390 too depleted in Sr to represent an appropriate assimilant. Instead, we suggest that the
391 assimilant could be MORB or FAB plagioclase-rich cumulates present in the lower crust.
392 Given that the Lesser Antilles arc is thought to be built on the Aves ridge (extinct arc)
393 forearc after a slab rollback that displaced the activity eastward, FAB cumulates are more
394 likely to be present at the base of the Lesser Antilles arc than MORB cumulates. Such
395 rocks would likely occur under every island and meet the geochemical requirements of

396 the assimilant described above. They could comprise mafic layers, but the more felsic
397 sections would be preferentially assimilated by primitive magmas. While the mafic layers
398 of cumulates tend to concentrate the iridium platinum group element (IPGE) because
399 these elements are removed from the melt early during differentiation and concentrate in
400 cumulus phases such as olivine or chromite, plagioclase-rich layers tend to concentrate
401 more Re (and palladium platinum group elements: PPGE) since it remain longer in the
402 melt and is more likely to be present as interstitial sulfides. Radiogenic Os, produced by
403 Re decay, is therefore more likely to be present in such layers. Since the Lesser Antilles
404 arc started accreting during the Oligocene (Germa et al., 2011), it would be predicted that
405 the early-arc FAB lavas and cumulates would have a moderately radiogenic $^{187}\text{Os}/^{188}\text{Os}$,
406 consistent with the signature of the assimilant. The mantle-like Sr isotopic composition of
407 the cumulate would also be consistent with their production early in the arc existence,
408 prior to significant fluids fluxing through the mantle.

409 Finally, none of the lavas analysed have a europium positive anomaly, the latter
410 being expected in the case of assimilation of large amounts of plagioclase. However, all
411 but one lava (STV301) contain plagioclase phenocrysts which indicate that plagioclase
412 fractionation may have erased any such positive anomaly. The absence of any Eu
413 anomaly in the plagioclase-free high-MgO basalt from St Vincent could be explained by
414 the low amount of assimilation involved in that lava (~ 7%; Fig. 6) or if the assimilated
415 plagioclase cumulates did not have a significant positive Eu anomaly. A low Eu anomaly
416 in plagioclase can only occur in highly oxidised magmas. Since the plagioclase cumulates
417 are likely to have crystallised at the initiation of the subduction zone, their oxygen
418 fugacity is likely to be similar to that of FAB erupted at the onset of the Mariana

419 subduction, which have been shown to present high oxygen fugacity (QFM +0.4;
420 Brounce et al., 2013), and are likely to crystallise plagioclase with small Eu anomalies.

421 *4.3.3 Assimilation and fractional crystallisation (AFC) modelling*

422 The AFC equation (DePaolo, 1981) can be used to model the $^{187}\text{Os}/^{188}\text{Os}$,
423 $^{87}\text{Sr}/^{88}\text{Sr}$, La/Sm and Sr/Th relationships using reasonable parameters (Figs. 6a, b, c). We
424 used the Grenada picrite (LAG4) for the initial magma composition, since it plots within
425 the mantle range in terms of $^{187}\text{Os}/^{188}\text{Os}$ and its Os concentration (360 ppt Os) is
426 consistent with that expected with a melt in equilibrium with sulfide-bearing mantle. The
427 range of Os, Sr, Th, La and Sm bulk partition coefficients (D) (Table 3) were estimated
428 by dividing the concentration of these elements in the Grenada picrite by their
429 concentration in the most differentiated samples. Sr, Th, La and Sm bulk D's obtained are
430 consistent with fractionation of the observed phenocryst assemblages (olivine \pm pyroxene
431 \pm plagioclase). The Os bulk partition coefficients used (D = 12-16) are in agreement with
432 that expected for \sim 0.5% of chromian-spinel fractionation (Chesley et al., 2002; Righter et
433 al., 2002). The $^{187}\text{Os}/^{188}\text{Os}$ ratio of the assimilant ($^{187}\text{Os}/^{188}\text{Os} = 0.245$) can be easily
434 produced by radiogenic ingrowth of a DMM composition with an initial ratio of
435 $^{187}\text{Os}/^{188}\text{Os}$ (0.127). This could occur within the 25 My since magmatism was initiated in
436 the Lesser Antilles (Germa et al., 2011), even if the initial $^{187}\text{Re}/^{188}\text{Os}$ is lower than
437 MORB (\sim 600). The Os concentration of the assimilant used in the model (20 ppt) is
438 consistent with that expected from a plagioclase-rich cumulate grown from the residual
439 melt of a MORB/FAB primitive magma (with \sim 350-200 ppt Os; derived from a sulfide-
440 bearing mantle) after fractionation of important amounts of olivine and spinel. Indeed 20
441 ppb Os is within the range of concentrations observed in the basalts with the lowest MgO

442 analysed in this study (5-44 ppt for MgO 5.1-8.7 wt.%), some of the latter presenting
443 phenocryst assemblages with up to 70% plagioclase and less than 20% olivine (e.g.
444 STV324; Heath et al. (1998)).

445 All data could be modeled using the same starting (LAG-4) and assimilant
446 composition (Table 3) and with $F > 0.8$. In $^{87}\text{Sr}/^{86}\text{Sr}$ vs. $^{187}\text{Os}/^{188}\text{Os}$ space, the lavas fall
447 on two trends produced by different rates of assimilation and small variations in D_{Sr} ($r =$
448 0.56 vs. 0.70 ; $D_{\text{Sr}} = 1.4$ - 1.8). On trace element ratio vs. isotope diagrams (Fig.6b, c), the
449 effect of variations in the fractionating assemblage during assimilation on different
450 islands (= variation in D) is reflected by small displacement of the samples on these
451 trends compared to isotope-isotope space (Fig. 6a). The north-south difference observed
452 in La/Sm vs. $^{187}\text{Os}/^{188}\text{Os}$ can be easily produced by increasing $D_{\text{La}/\text{Sm}}$. We suggest that
453 such north-south variations in $D_{\text{La}/\text{Sm}}$ could be related to the depth at which AFC occurs.
454 In this case, the assemblage fractionated during assimilation in the north of the arc
455 depleted La less than the assemblage fractionated in the south for a constant D_{Sm} . For
456 example, it would be the case if, during assimilation, the fractionated assemblage is
457 dominated by olivine ($D_{\text{La}/\text{Sm}} \sim 1$) in the south of the arc and by clinopyroxene ($D_{\text{La}/\text{Sm}} < 1$)
458 in the north of the arc. Such variations in the fractionating assemblage composition would
459 have negligible effect on the isotopic composition of the lavas, consistent with the single
460 trend observed in Sr vs Os isotopes from north to south.

461 **4.4 Implications**

462 *4.4.1 The Lesser Antilles*

463 Although assimilation of sediment (high $\delta^{18}\text{O}$, $^{87}\text{Sr}/^{86}\text{Sr}$, $^{208-207-206}\text{Pb}/^{204}\text{Pb}$ and low
464 $^{176}\text{Hf}/^{177}\text{Hf}$ and $^{143}\text{Nd}/^{144}\text{Nd}$ ratios) had been shown to modify some lava compositions in
465 the central-southern part of the arc (Thirlwall and Graham, 1984; Davidson, 1987;
466 Davidson and Harmon, 1989; Smith et al., 1996; Thirlwall et al., 1996; Van Soest et al.,
467 2002; Bezard et al., 2014), assimilation of another component in the deep crust of the
468 Lesser Antilles arc (Fig. 7) was not anticipated and differences between the Grenada
469 picrite compositions and the rest of the arc lavas have traditionally been attributed to
470 differences in source composition. This work suggests that the Grenada picrites might
471 provide the only close estimates of the source composition in terms of $^{87}\text{Sr}/^{86}\text{Sr}$,
472 $^{187}\text{Os}/^{188}\text{Os}$, Sr and REE. Thus, the use of such proxies in less primitive lavas to constrain
473 the relative contributions of fluids versus sediment in the arc source may need
474 reappraisal. All the arc data seem to back-project toward a primitive magma with the
475 Grenada picrite composition (Fig. 4) although small variations in the source from north to
476 south can't be precluded. The investigation of such variations is, however, hampered by
477 the absence of very mafic lavas, such as those found in St Vincent and Grenada, in the
478 northern arc. Since the Grenada picrite is the only silica undersaturated lavas, this
479 suggests that primitive magma along the arc in general could be of a similar alkaline
480 nature before AFC, as suggested by Macdonald et al. (2000). The absence of cumulate
481 assimilation by Grenada picrites could be either due to a lack of significant amount of
482 cumulate at the base of the arc crust, or to the presence of crustal structures allowing the
483 magma to reach the surface with minimal stalling at the base of the crust. The latter
484 hypothesis could be supported by the presence of a transform fault in Grenada, which has
485 been suggested to control the emplacement of the most recent products (Arculus, 1976).

486 4.4.2 Other arcs

487 The correlation between Os (or 1/Os) and $^{187}\text{Os}/^{188}\text{Os}$ observed in the Lesser
488 Antilles arc is not unique and has been noted in most continental and oceanic arc lavas
489 (Fig. 8a; Alves et al., 1999; 2002; Borg et al., 2000; Chesley et al. 2002; Woodland et al.,
490 2002; Woodhead et al., 2004; Turner et al., 2009; Righter et al., 2012). However, clear
491 correlations between Os isotopes and both Os concentrations and indices of
492 differentiation (MgO, SiO₂) have only been noted in continental arcs (Lassiter and Luhr,
493 2001; Chesley et al., 2002). The absence of clear MgO-SiO₂ correlations with $^{187}\text{Os}/^{188}\text{Os}$
494 in oceanic arc lavas (Fig. 8b) led previous studies to suggest source control of the inverse
495 correlation between Os concentration and $^{187}\text{Os}/^{188}\text{Os}$ (Alves et al., 1999). Our Lesser
496 Antilles study suggests that the correlations between $^{187}\text{Os}/^{188}\text{Os}$ and Os content and the
497 “radiogenic $^{187}\text{Os}/^{188}\text{Os}$ ratios observed in oceanic arcs could reflect crustal assimilation
498 and that slab-derived Os may not be transferred into the magma source regions, as
499 proposed by Righter et al. (2012). It also suggests, based on the radiogenic $^{187}\text{Os}/^{188}\text{Os}$
500 ratio in the St Vincent high-MgO lavas (MgO = 12.6 wt. %), that the process can affect
501 very primitive magmas. Although the conditions of assimilation may be different in every
502 arc, early assimilation during differentiation could explain the radiogenic $^{187}\text{Os}/^{188}\text{Os}$
503 observed in early crystallizing phases such as Cr-spinel in Bonin Islands tholeiites
504 (Suzuki et al, 2011).

505 Unlike the correlation between Os isotopes and Os concentrations, the covariation
506 of Os isotopes with lithophile isotope or trace element ratios observed in the Lesser
507 Antilles (e.g. Sr isotopes, Sr/Th and La/Sm) is not ubiquitous in other arcs (e.g. Fig. 8c,
508 d), with only the Cascades lavas showing similarly clear correlations between $^{187}\text{Os}/^{188}\text{Os}$

509 and $^{87}\text{Sr}/^{86}\text{Sr}$ ratios and Sr concentrations (Borg et al., 2000; Fig. 8c, d). This lack of
510 obvious co-variation could be explained by more limited compositional differences
511 between the primary magma and the assimilant which would rend the impact of
512 assimilation harder to observe. Indeed, in the Lesser Antilles, the $^{87}\text{Sr}/^{86}\text{Sr}$, Sr/Th and
513 La/Sm ratios of the primitive magmas differs significantly from those of the assimilant,
514 which results in obvious mixing lines. However, the $^{87}\text{Sr}/^{86}\text{Sr}$, Sr/Th and La/Sm ratios of
515 primitive magmas are likely to vary with the composition of the subducted sediment and
516 as demonstrated in Fig. 8c and 8d, the very ‘continental’ isotopic and trace element
517 signature of the Lesser Antilles primitive magma is not commonly observed in other
518 oceanic arcs, the latter presenting composition closer to MORB (e.g. picrites from the
519 Vanuatu or Salomon islands have $^{87}\text{Sr}/^{86}\text{Sr} \sim 0.703\text{-}0.7045$ contrasting with the $^{87}\text{Sr}/^{86}\text{Sr}$
520 of ~ 0.7051 of the most primitive picrite in Grenada; Peate et al., 1997; Schuth et al.,
521 2004). Therefore, assimilation of a recent FAB like cumulate by primitive magmas would
522 be much harder to detect in most oceanic arcs than in the Lesser Antilles. In addition, the
523 rocks assimilated in other arcs might have lower Sr concentrations, rending the impact of
524 the process on Sr/Th and $^{87}\text{Sr}/^{86}\text{Sr}$ hard to fingerprint. Alternatively, along-arc primitive
525 magma compositional variations may exist, interfering with the variations produced by
526 assimilation.

527 **5. CONCLUSIONS**

528 Our observations suggest that no significant slab derived Os is present in the
529 primitive magmas of the Lesser Antilles arc. We interpret the increase in Os isotopic
530 ratios observed in the lavas as caused by crustal assimilation in the deep crust of the arc.
531 The assimilant would be similar all along the arc and display lower $^{87}\text{Sr}/^{86}\text{Sr}$ (MORB-

532 like), La/Sm and higher $^{187}\text{Os}/^{188}\text{Os}$, Sr and Sr/Th than the primitive magma. We suggest
533 that it could be a plagioclase-rich cumulate present at the base of the arc. Such cumulate
534 could have been produced during the early-arc stage, prior to significant amount of
535 fluids/sediments fluxing in the mantle.

536 **ACKNOWLEDGEMENTS**

537 Financial support was provided to Rachel Bezar by Durham and Macquarie
538 University cotutelle studentship (No. 2012060). We thank Peter Wieland for his help
539 during the analytical work and we thank Matthijs C. van Soest for providing some of the
540 samples.

541 **REFERENCES**

- 542 Alves, S., Schiano, P. and Allegre, C.J. (1999) Rhenium-osmium isotopic investigation of
543 Java subduction zone lavas. *Earth Planet. Sci. Lett.* **168**, 65-77.
- 544 Alves, S., Schiano, P., Capmas, F. and Allegre, C.J. (2002) Osmium isotope binary
545 mixing arrays in arc volcanism. *Earth Planet. Sci. Lett.* **198**, 355-369.
- 546 Arculus, R. (1976) Geology and geochemistry of the alkali basalt-andesite association of
547 Grenada. Lesser Antilles island arc. *Geol. Soc. Am. Bull.* **87**, 612-624.
- 548 Bezar, R., Davidson, J.P., Turner, S., Macpherson, C.G., Lindsay, J.M. and Boyce, A.J.,
549 (2014) Assimilation of sediment embedded in oceanic arc crust: myth or reality? *Earth*
550 *Planet. Sci. Lett.* **395**, 51-60.
- 551 Baker, P.E. (1984) Geochemical evolution of St Kitts and Montserrat, Lesser Antilles. *J.*
552 *Geol. Soc. Lond.* **141**, 401-411.

553 Borg, L.E., Brandon, A.D., Clyne, M.A. and Walker, R.J. (2000) Re-Os isotopic
554 systematics of primitive lavas from the Lassen region of the Cascade Arc, California.
555 *Earth Planet. Sci. Lett.* **177**, 301-317.

556 Boynton, C.H., Westbrook, G.K., Bott, M.H.O. and Long, R.E., 1979. A seismic
557 refraction investigation of crustal structure beneath the Lesser Antilles island arc.
558 *Geophys. J. R. Astron. Soc.* **58**, 371-393.

559 Brandon, A.D. and Draper, D.S. (1996) Constraints on the origin of the oxidation state of
560 the mantle overlying subduction zones: an example from Simcoe, Washington, USA.
561 *Geochim. Cosmochim. Acta* **60**, 1739-1749.

562 Brandon, A.D., Creaser, R.A., Shirey, S.B. and Carlson, R.W. (1996) Os recycling in
563 subduction zones. *Science* **272**, 861-864.

564 Brounce, M.N., Kelley, K. and Cottrell, E. (2013) Temporal evolution of fO_2 in the
565 Mariana mantle wedge. *American Geophysical Union abstract*.

566 Carpentier, M., Chauvel, C. and Mattielli, N. (2008) Pb-Nd isotopic constraints on
567 sedimentary input into the Lesser Antilles arc system. *Earth Planet. Sci. Lett.* **272**, 199-
568 211.

569 Chesley, J., Ruiz, J., Richter, K., Ferrari, L. and Gomez-Tuena, A. (2002) Source
570 contamination versus assimilation: an exemple from the Trans-Mexican Volcanic Arc.
571 *Earth Planet. Sci. Lett.* **195**, 211-221.

572 Cohen, A.S. and Waters, F.G. (1996) Separation of osmium from geological materials by
573 solvent extraction for analysis by thermal ionisation mass spectrometry. *Anal. Chim. Acta*
574 **332**, 269-275.

575 Creaser, R.A., Papanastassiou, D.A. and Wasserburg, G.J. (1991) Negative thermal ion
576 mass spectrometry of osmium, rhenium and iridium. *Geochim. Cosmochim. Acta* **55**, 397-
577 401.

578 Davidson, J.P. (1984) Petrogenesis of Lesser Antilles island arc magmas: Isotopic and
579 geochemical constraints. *PhD thesis, Uni. Leeds*, 308 pp.

580 Davidson, J.P. (1986) Isotopic and trace element constraints on the petrogenesis of
581 subduction-related lavas from Martinique, Lesser Antilles. *J Geophys. Res.* **91**, 5943-
582 5962.

583 DePaolo, D.J. (1981) Trace element and isotopic effects of combined wall rock
584 assimilation and fractional crystallization. *Earth Planet. Sci. Lett.* **53**, 189-202.

585 Dufrane, S.A., Turner, S., Dosseto, A. and Van Soest, M. (2009) Reappraisal of fluid and
586 sediment contributions to Lesser Antilles magmas. *Chem. Geol.* **265**, 272-278.

587 Germa, A., Quidelleur, X., Labanieh, S., Chauvel, C. and Lahitte, P. (2011) The Volcanic
588 evolution of Martinique Island: Insights from K-Ar dating into the Lesser Antilles arc
589 migration since the Oligocene. *J. volcano. Geoth. Res.* **208**, 122-135.

590 Hart, S.R. and Davis, K.E. (1978). Nickel partitioning between olivine and silicate melt.
591 *Earth and Planet. Sci.* **40**, 203-209.

592 Hayes, D.E., et al. (1972) Initial Reports of the Deep Sea Drilling Project 14. U.S.
593 Government Printing Office, Washington.

594 Heath, E., Macdonald, R., Belkin, H., Hawkesworth, C. and Sigurdsson, H. (1998)
595 Magmagenesis at Soufriere Volcano, St Vincent, Lesser Antilles Arc. *J. Petrology* **39**,
596 1721-1764.

597 Kendall, B., Creaser, R.A. and Selby, D. (2009) ^{187}Re - ^{187}Os geochronology of
598 Precambrian organic-rich sedimentary rocks. *Geol. Soc. London Spec. Pub.* **326**, 85-107.

599 Le Guen de Kerneizon, M., Carron, J.P., Bellon, H. and Maury, R.C. (1981). Enclaves
600 metamorphiques et plutoniques, provenant du substratum des Petites Antilles, dans les
601 formations volcaniques de l'île de Sainte Lucie. *CR Acad. Sci. Paris* **292**, 899-902.

602 Macdonald, R., Hawkesworth, C.J. and Heath, E. (2000) The Lesser Antilles volcanic
603 chain: a study in arc magmatism. *Earth Sci. Rev.* **49**, 1-76.

604 McInnes, B.I.A., McBride, J.S., Evans, N.J., Lambert, D.D. and Andrew, A.S. (1999)
605 Osmium Isotope Constraints on Ore Metal Recycling in Subduction zones. *Science* **286**,
606 512.

607 Nowell, G.M., Luguet, A., Pearson, D.G. and Horstwood, M.S.A. (2008). Precise and
608 accurate $^{186}\text{Os}/^{188}\text{Os}$ and $^{187}\text{Os}/^{188}\text{Os}$ measurements by multi-collector plasma ionisation
609 mass spectrometry (MC-ICP-MC) part I: Solution analyses. *Chem. Geol.* **248**, 363-393.

610 Parkinson, J.J., Hawkesworth, C.J. and Cohen, A.S. (1998) Ancient mantle in a modern
611 arc: osmium isotopes in Izu-Bonin-Mariana forearc peridotites. *Science* **281**, 2011-2013.

612 Peate, D.W., Pearce, J.A., Hawkesworth, C.J., Colley, H., Edwards, C.M.H. and Hirose,
613 K. (1997) Geochemical variations in Vanuatu Arc lavas: the role of the subducted
614 material and a variable mantle wedge composition. *J. petrol.* **38**, 1331-1358.

615 Penniston-Dorland, S.C., Walker, R.J., Pitcher, L., Sorensen, S.S. (2012) Mantle-crust
616 interactions in a paleosubduction zone: Evidence from a highly siderophile element
617 systematics of eclogite and related rocks. *Earth Planet. Sci. Lett.* **319-320**, 295-306.

618 Penniston-Dorland, S.C., Gorman, J.K., Bebout, G.E., Piccoli, P.M. and Walker, R.J.
619 (2014) Reaction rind formation in the Catalina Schist: Deciphering a history of
620 mechanical mixing and metasomatic alteration. *Chem. Geol.* **384**, 47-61.

621 Peucker-Ehrenbrink, B. and Ravizza, G. (2000) The marine osmium isotope record.
622 *Terra Nova* **12**, 205-219.

623 Reagan, M.K., Ishizuka, O., Stern, R.J., Kelley, K.A., Ohara, Y. et al. (2010) Fore-arc
624 basalts and subduction initiation in the Izu-Bonin-Mariana system. *Geochem. Geophys.*
625 *Geosyst.* **Q03X12**, doi: 10.1029/2009GC002871.

626 Richter, K., Chesley and J.T. and Ruiz, J. (2002) Genesis of primitive, arc type basalt:
627 Constraints from Re, Os, and Cl on the depth of melting and role of fluids. *Geology* **30**,
628 619-622.

629 Rudnick, R. and Walker, R.J. (2009) Interpreting ages from Re-Os isotopes in peridotites.
630 *Lithos* **102S**, 1083-1095.

631 Saal, A.E., Rudnick, R.L., Ravizza, G.E. and Hart, S.R. (1998) Re-Os isotope evidence
632 for the composition, formation and age of the lower continental crust. *Lett. Nature* **393**,
633 58-61.

634 Salters, V.J.M. and Stracke, A. (2004) Composition of the depleted mantle. *Geochem.*
635 *Geophys. Geosyst* **Q05B07**, doi: 10.1029/2003GC000597.

636 Schuth, S., Rohrbach, A., Munker, C., Ballaus, C., Garbe-Schonberg, D. and Qopoto, C.
637 (2004) Geochemical constraints on the petrogenesis of arc picrites and basalts, New
638 Georgia Group, Solomon Islands. *Contrib. Mineral. Petrol.* **148**, 288-304.

639 Selby, D. and Creaser, R.A. (2003) Re-Os geochronology of organic-rich sediments: an
640 evaluation of organic matter analysis methods. *Chem. Geol.* **200**, 225-240.

641 Sun, S.S. and McDonough, W.F. (1989) Chemical and isotopic systematics of oceanic
642 basalts: implications for mantle composition and processes. *Geol. Soc. Lond.* **42**, 313-
643 345.

644 Suzuki, K., Senda, R. and Shimizu, K. (2011) Osmium behaviour in a subduction system
645 elucidated from chromian spinel in Bonin Island beach sands. *Geology* **39**, 999-1002.

646 Senda, R., Tanaka, T. and Suzuki, K. (2007) Os, Nd and Sr isotopic and chemical
647 compositions of ultramafic xenoliths from Kurose, SW Japan: Implications for
648 contribution of slab-derived material to wedge mantle. *Lithos* **95**, 229-242. Turner, S.,
649 Handler, M., Bindeman, I. and Suzuki, K. (2009) New insights into the origin of O-Hf-Os
650 isotope signatures in arc lavas from Tonga-Kermadec. *Chem. Geol.* **266**, 187-193.

651 Thirlwall, M.F., Graham, A.M., Arculus, R.J., Harmon, R.S. and Macpherson, C.G.
652 (1996) Resolution of the effects of crustal assimilation, sediment subduction and fluid
653 transport in island arc magmas: Pb-Sr-Nd-O isotope geochemistry of Grenada, Lesser
654 Antilles. *Geochim. Cosmochim. Acta* **60**, 4785-4810.

655 Turgeon, S. and Creaser, R.A. (2008) Cretaceous oceanic anoxic event 2 triggered by a
656 massive magmatic episode. *Nature* **454**, 323-326.

657 Van Soest, M. C. (2000) Sediment Subduction and Crustal contamination in the Lesser
658 Antilles Island Arc. PhD thesis Uni. Vrije, 287 pp.

659 Volkening, J., Walczyk, T. and Heumann, K.G. (1991) Osmium isotope ratio
660 determinations by negative thermal ionization mass spectrometry. *Int. J. Mass Spec. Ion*
661 *Process.* **105**, 147-159.

662 Widom, E., Kepezhinskas, P. and Defant, M. (2003) The nature of metasomatism in the
663 sub-arc mantle wedge: evidence from Re-Os isotopes in Kamchatka peridotite xenoliths.
664 *Chem. Geol.* **196**, 283-306.

665 Woodhead, J. and Brauns, M. (2004) Current limitations to the understanding of Re-Os
666 behaviour in subduction systems, with an exemple from New Britain. *Earth Planet. Sci.*
667 *Lett.* **221**, 309-323.

668 Woodland, S.J., Pearson, D.G. and Thirlwall, M.F. (2002) A Platinum Group Element
669 and Re-Os Isotope Investigation of Siderophile Element Recycling in Subduction Zones:
670 Comparison of Grenada, Lesser Antilles Arc, and the Izu-Bonin Arc. *J. Petrol.* **43**, 171-
671 198.

672 Xiong, Y. and Wood, S.A. (1999) Experimental determination of the solubility of ReOs
673 and the dominant oxidation state of rhenium in hydrothermal systems. *Chem. Geol.* **158**,
674 245-256.

675 Xiong, Y. and Wood, S.A. (2000) Experimental quantification of hydrothermal solubility
676 of platinum group elements with special reference to porphyry copper environments.
677 *Mineral. Petrol.* **68**, 1-28.

678 **Figure captions:**

679 Fig. 1: Map of the Lesser Antilles arc with the location of selected lava samples (in
680 black). One sample from each island (except St. Vincent, n=2) was analysed. See Table 1
681 for sample identification. The latitude of DSDP sites 543/543A and 144 are also
682 indicated.

683 Fig. 2: $^{87}\text{Sr}/^{86}\text{Sr}$ vs. (a) $^{143}\text{Nd}/^{144}\text{Nd}$, (b) MgO (wt. %), (c) La/Sm and (d) Sr/Th of the
684 lavas selected. Data presented in Table 2.

685 Fig. 3: Os (ppb) vs. $^{187}\text{Os}/^{188}\text{Os}$ of the arc lavas and the subducting slab. DMM =
686 Depleted MORB mantle from Rudnick and Walker (2009). Note logarithmic scales. Data
687 presented in Table 1.

688 Fig. 4: Lavas Os (ppb) and MgO (wt. %) against $^{187}\text{Os}/^{188}\text{Os}$. Same legend as in figure 3.
689 The same negative correlation is also observed between $^{187}\text{Os}/^{188}\text{Os}$ and Mg#. Woodland
690 et al. (2002) data on different Grenada lavas are shown for comparison. Arrows shows
691 potential differentiation trends for the northern and southern islands, starting with the
692 most primitive lava of the arc.

693 Fig. 5: (a) $^{87}\text{Sr}/^{86}\text{Sr}$, (b) La/Sm and (c) Sr/Th vs $^{187}\text{Os}/^{188}\text{Os}$ composition of the lavas.
694 Subducting slab composition are also indicated. Data for arc lavas and sediment and
695 altered basalt from the slab are presented in Tables 1 and 3. DMM = depleted mantle
696 from Rudnick and Walker (2009) for Os isotopes and Salters and Stracke (2004) for Sr.
697 isotopes; Lower continental crust composition is from Saal et al. (1999), N-MORB trace
698 element composition is from Sun and McDonough (1989). Arrows highlight the negative
699 trends drawn by the data.

700 Fig. 6: Assimilation during Fractional Crystallization (AFC) models of (a,b) $^{87}\text{Sr}/^{86}\text{Sr}$,
701 (a,c) $^{187}\text{Os}/^{188}\text{Os}$, (b) Sr/Th and (c) La/Sm ratios of the Lesser Antilles primitive lavas
702 using DePaolo (1981) equation. Parameters for Models 1 and 2 are shown in Table 3.
703 Dots represent the fraction of melt remaining (F). In (b) and (c), samples with
704 compositions displaced from their position on the trends defined in the isotope-isotope
705 space (a) (likely due to the impact of mineral fractionation) are circled. The arrows show
706 the inferred compositions before displacements.

707 Fig. 7: Schematic model for the Lesser Antilles plumbing system to explain the main
708 factors influencing the compositional variations of the arc lavas. The figure illustrates
709 both the locus (cartoon) and the impact (diagrams) of cumulate assimilation on the lava's
710 $^{187}\text{Os}/^{188}\text{Os}$, $^{87}\text{Sr}/^{86}\text{Sr}$, La/Sm and $\delta^{18}\text{O}$ compositions (evolution of Sr/Th ratio is not
711 shown). The impact of subsequent assimilation of sediment (Bezard et al., 2014), which
712 is not discussed in this contribution, is also shown for a full illustration of the arc
713 processes. The arc primary magmas would come from a source strongly influence by the
714 subducted sediment. Grenada picrite (A) would have avoided any storage in the arc crust
715 and retained the primitive magma composition. All the less primitive lavas (B) would

716 have spent variable amounts of time in contact with a plagioclase-rich cumulate in the
717 lower parts of the crust. The resulting magmas would have either ascended directly to the
718 surface (B) or assimilated some sediment during the ascent (C). M = mantle composition.

719 Fig. 8: Comparison of the Lesser Antilles arc lava compositions with those of other arcs
720 (continental and oceanic). The negative correlation observed between Os isotopes and Os
721 concentrations is ubiquitous in arcs (a). On the other hand, negative correlations between
722 Os isotopes and MgO (b) or Sr isotopes (c) as well as a positive correlation between
723 Sr/Th and Os isotopes (d) are not observed in every arcs. Lava compositions are from
724 Borg et al., (2000) for the Cascades, Chesley et al. (2002) for the Trans-Mexican arc,
725 Turner et al. (2009) for the Tonga-Kermadec, Alves et al. (1999) for Java, Woodhead and
726 Brauns (2004) for New Britain and Woodland et al. (2002) for the additional Lesser
727 Antilles arc data.

728

Fig. 1

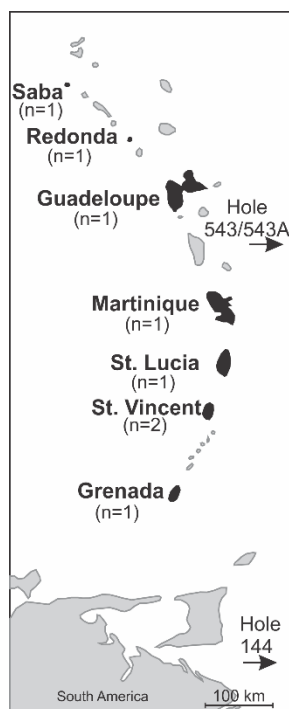


Fig. 2

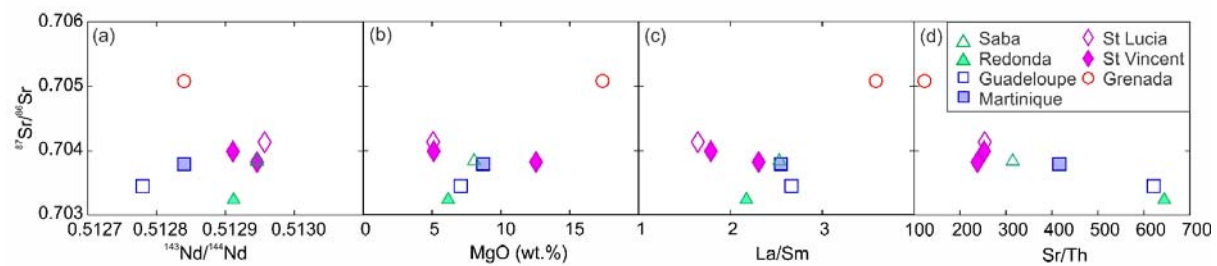


Fig. 3

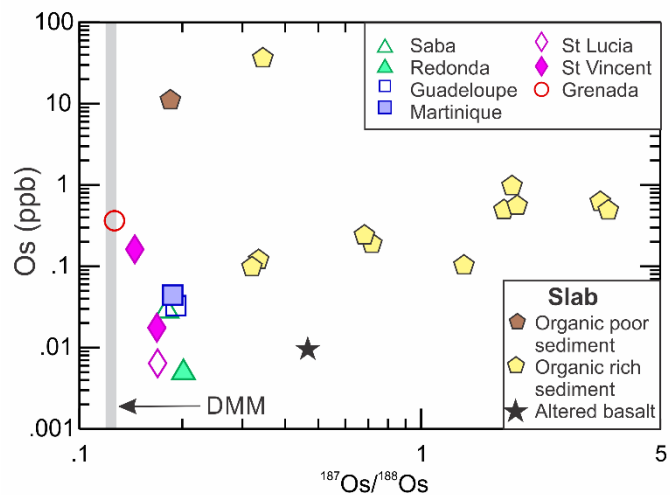


Fig. 4

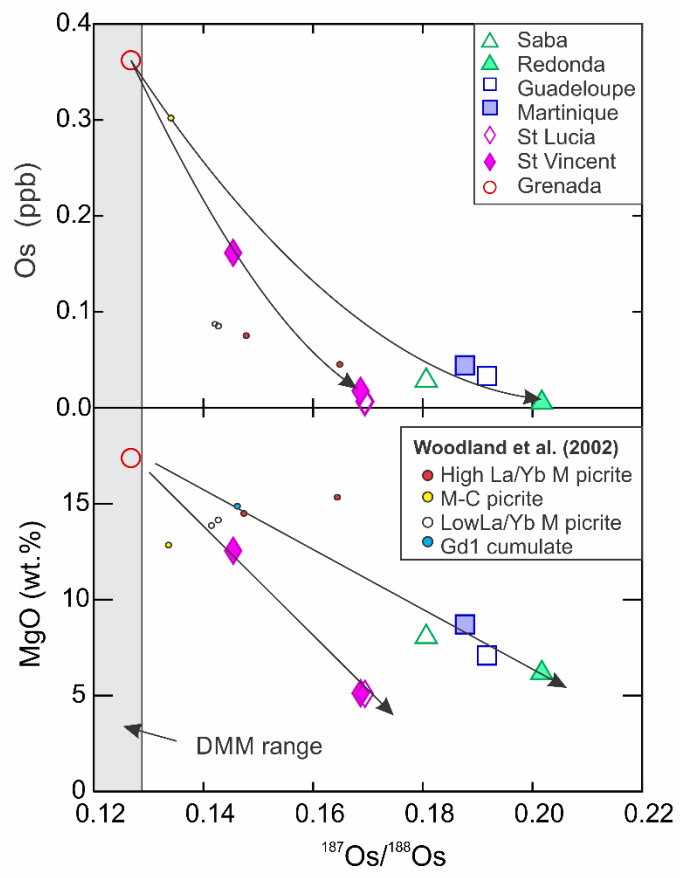


Fig. 5

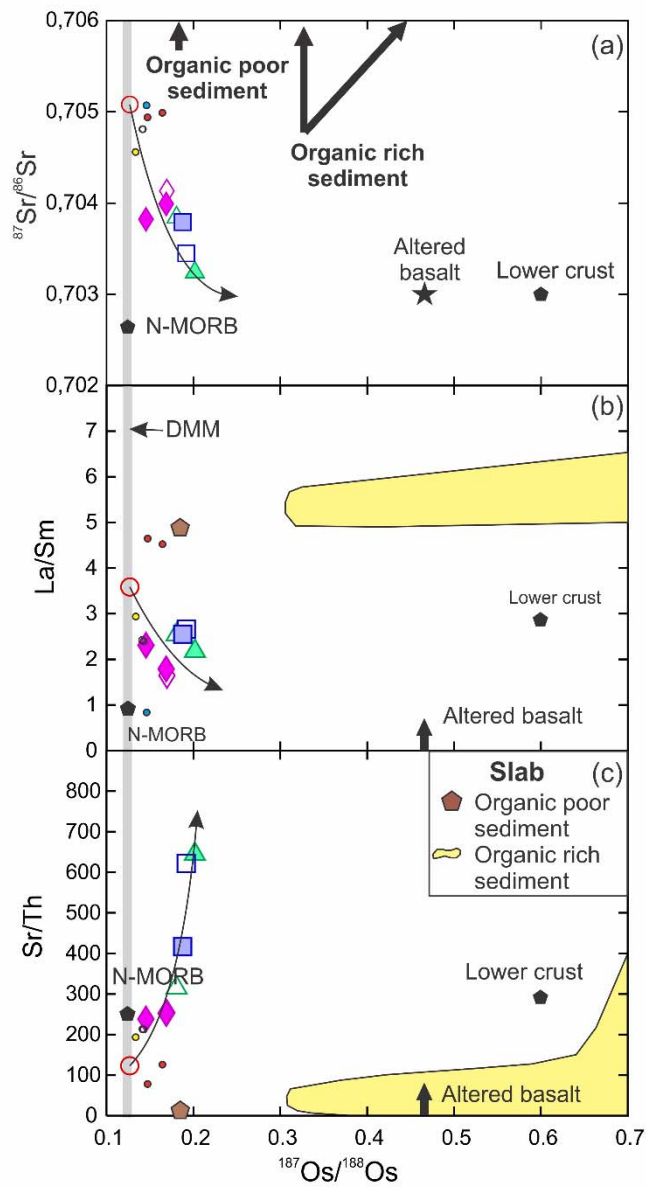


Fig. 6

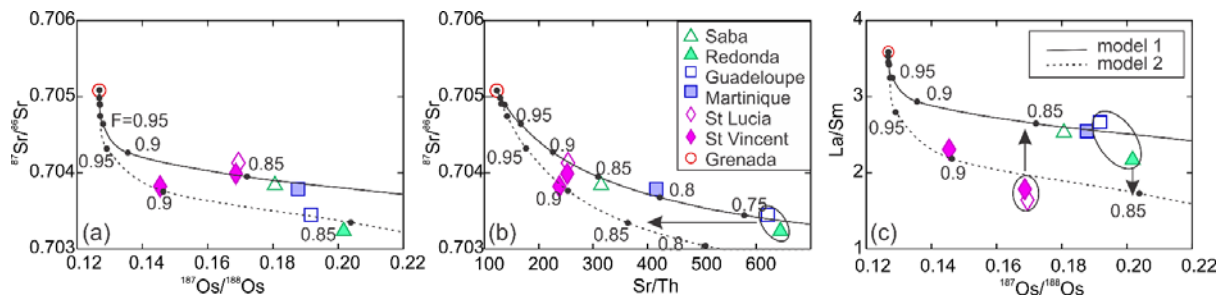


Fig. 7

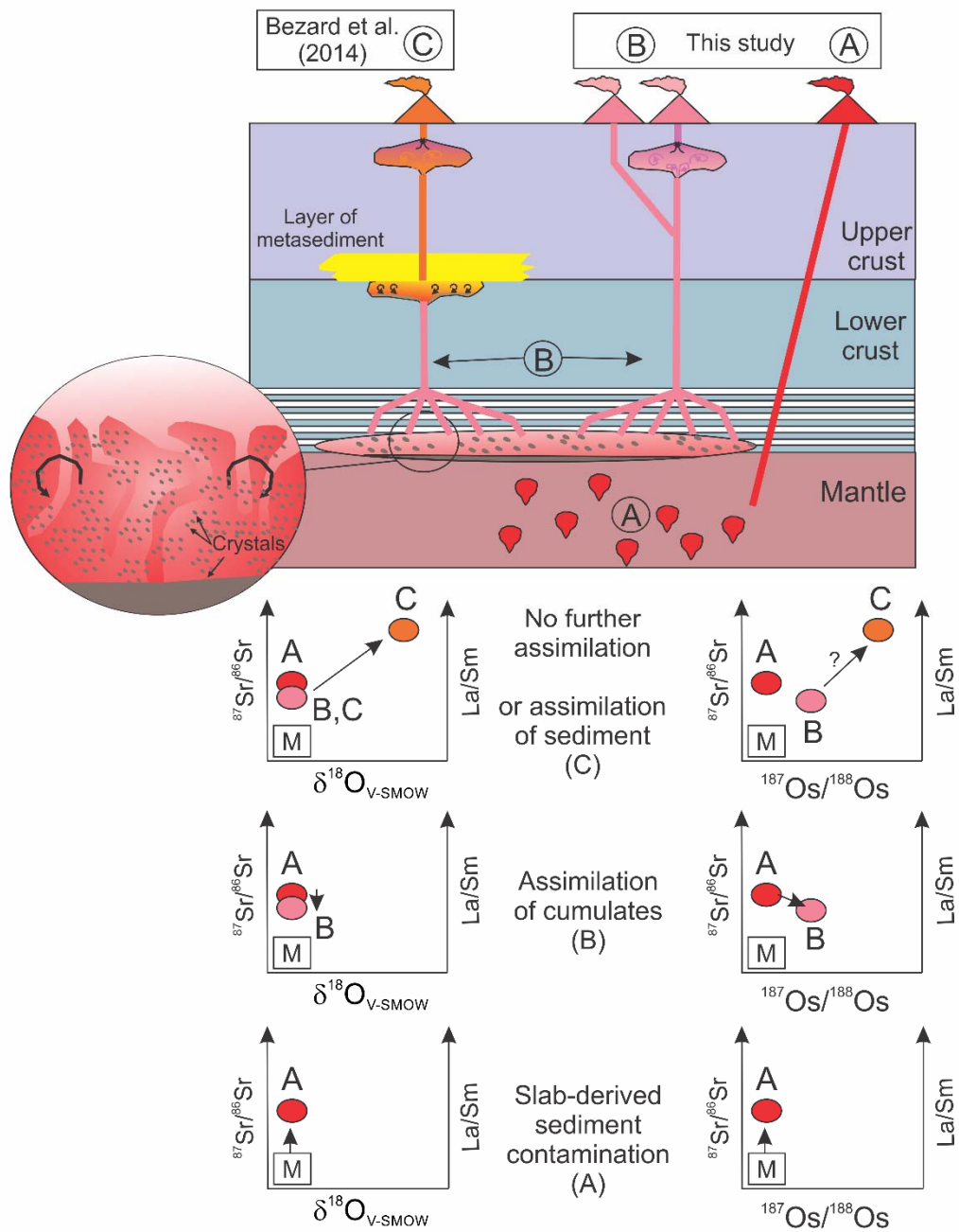


Fig. 8

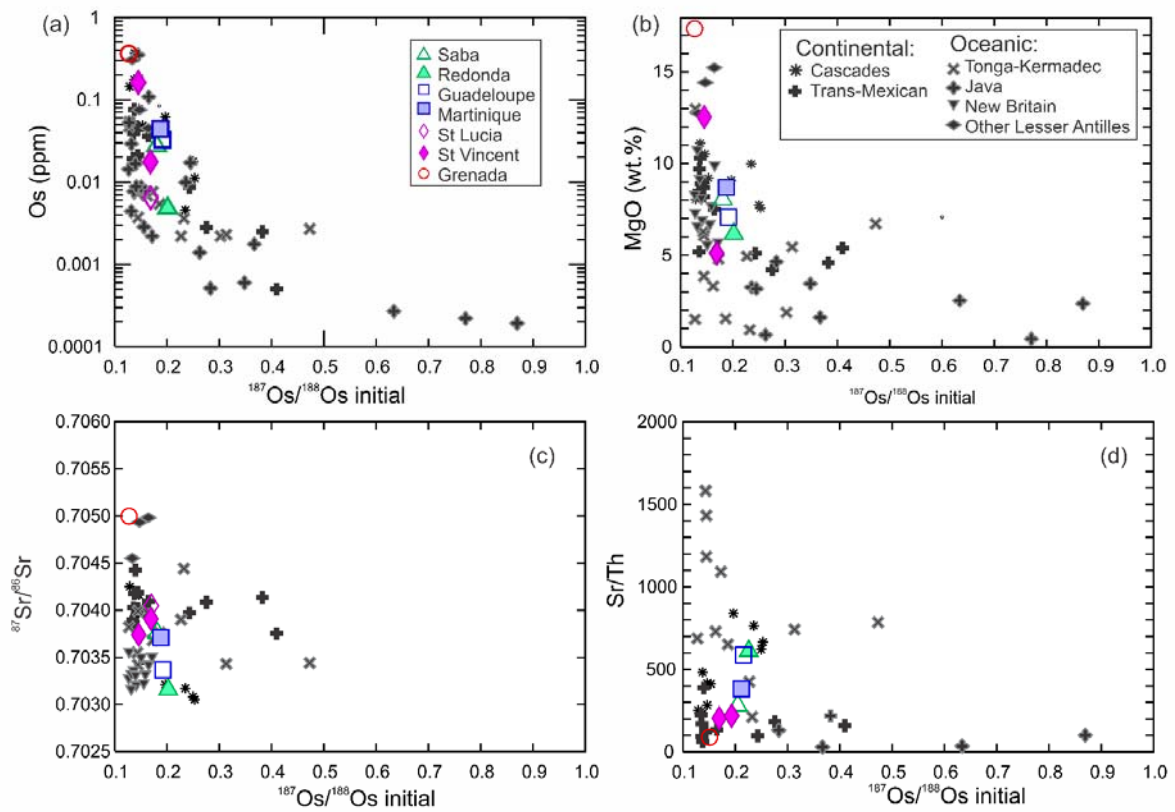


Table 1: Os data for the arc lavas and altered basalt and sediments from the subducting slab.

	Subbottom depth (m)	Lithology Unit #	Os (ppb)	±	¹⁸⁷ Os/ ¹⁸⁸ Os	±	¹⁸⁷ Re/ ¹⁸⁸ Os	±	Re (ppb)	±	Age (ka) ^d	¹⁸⁷ Os/ ¹⁸⁸ Os initial
Lavas (from N to S):												
Saba-LAS1 ^a	–	–	0.0281	0.0001	0.181	0.001	–	–	–	–	<10	–
Redonda-R8204 ^a	–	–	0.0049	0.0001	0.202	0.002	–	–	–	–	1000	–
Guadeloupe-GUAD510 ^a	–	–	0.0328	0.0004	0.192	0.001	–	–	–	–	500	–
Martinique-M8328 ^a	–	–	0.0441	0.0002	0.188	0.001	–	–	–	–	<1000	–
St Lucia-SL8344 ^a	–	–	0.0064	0.0001	0.170	0.005	–	–	–	–	11400	–
St Vincent-STV301 ^a	–	–	0.161	0.001	0.1451	0.0007	–	–	–	–	180	–
St Vincent-STV324 ^a	–	–	0.0175	0.0001	0.169	0.002	–	–	–	–	<3.6	–
Grenada-LAG4 ^a	–	–	0.362	0.001	0.1268	0.0004	–	–	–	–	<10	–
Altered basalt 543 16 5 20-24 ^a	–	–	0.0096	0.0002	0.466	0.003	–	–	–	–	–	–
Sediments (increasing depth):												
Site DSDP 543												
78A-543-17-3-120-124 ^b	166	3	11.2	0.4	0.185	0.007	–	–	–	–	16000	–
Site DSDP 144/144A												
14-144A-5-1 interval 123-124 ^c	181	3	0.1009	0.0008	1.33	0.02	389	5	7.03	0.03	85000	0.78
14-144A-6-1 interval 70-110 ^c	189	3	0.941	0.003	1.844	0.005	721	3	115.0	0.4	89000	0.77
14-144Z-4-2 interval 60-64 ^c	215	3	0.478	0.003	3.52	0.02	1494	8	102.8	0.3	93000	1.21
14-144Z-4-2 interval 143-146 ^c	216	3	0.602	0.003	3.34	0.01	1425	6	125.4	0.4	93000	1.13
14-144Z-4-3 interval 31-33 ^c	216	3	0.534	0.002	1.913	0.006	755	3	67.8	0.2	93000	0.74
14-144Z-4-3 interval 100-103 ^c	217	3	0.484	0.002	1.746	0.007	580	3	48.1	0.2	93000	0.85
14-144Z-5-1 interval 5-6 ^c	264	4	0.231	0.001	0.682	0.008	178	2	7.93	0.03	98000	0.39
14-144Z-5-1 interval 143-143 ^c	265	4	0.186	0.002	0.72	0.02	164	3	5.89	0.02	98000	0.45
14-144Z-7-1 interval 136-137 ^c	299	5	0.116	0.001	0.34	0.01	32.3	0.7	0.757	0.007	106000	0.28
14-144Z-7-1 interval 123-124 ^c	299	5	34.5	0.3	0.34	0.01	122	3	847	3	106000	0.13
14-144Z-8-3 interval 136-137 ^c	328	5	0.0934	0.0005	0.321	0.005	16.7	0.7	0.32	0.01	113000	0.29

^a Os, ¹⁸⁷Os/¹⁸⁸Os analysed at Macquarie University.

^b Organic poor sediment: Os, ¹⁸⁷Os/¹⁸⁸Os analysed at Macquarie University.

^c Organic rich sediment: Os, ¹⁸⁷Os/¹⁸⁸Os, Re analysed at Durham University

^d Ages of Lava flows were taken from the following sources: Saba (Dufrane et al. 2009); Redonda (Baker, 1984); Guadeloupe (Dufrane et al., 2009); Martinique, Carbet Complex (Germa et al. (2011); St Lucia, Anse Galet (Le Guen de Kerneizon et al. (1983); St Vincent (Heath et al. (1998); Grenada (Dufrane, 2009). Ages indicated for the sediments, also used to calculate the initial ¹⁸⁷Os/¹⁸⁸Os ratios, correspond to that of the samples analysed by Carpentier et al. (2008; 2009) named in Table 2.

Note: Uncertainties are given as 2 sigma. For the latter the uncertainty includes the 2SE uncertainty for mass spectrometer analysis plus uncertainties for Os blank abundance and isotopic composition. The external reproducibility for ¹⁸⁷Os/¹⁸⁸Os and Os in lavas and organic-poor sediment, based on replicate analyses of WPR-1, is 1% and 4%, respectively. The external reproducibility for ¹⁸⁷Os/¹⁸⁸Os, ¹⁸⁷Re/¹⁸⁸Os, Os and Re in organic rich sediments, based on replicate analyses of SDO-1, is 7%, 7%, 16% and 15% respectively (see section 2.2).

Table 2: Lithophile major and trace element concentrations and isotopes of the arc lavas and altered basalt and sediments from the subducting slab analysed.

	Sample used for sediment lithophile element compositions (Carpentier et al., 2008;2009)	Subbotom Depth	MgO (wt. %)	Mg#	Sr (ppm)	La (ppm)	Sm (ppm)	Th (ppm)	⁸⁷ Sr/ ⁸⁶ Sr	¹⁴³ Nd/ ¹⁴⁴ Nd	
<u>Lavas (from N to S):</u>											
	Saba-LAS1 ^a	–	8.05	0.82	321	5.8	2.29	1.02	0.70384	0.51295	
	Redonda-R8204 ^a	–	6.17	0.74	493	4	1.84	0.77	0.70324	0.51291	
	Guadeloupe-GUAD510 ^a	–	7.08	0.76	261	3.7	1.4	0.42	0.70345	0.51278	
	Martinique-M8328 ^a	–	8.71	0.83	358	5.2	2.04	0.86	0.70379	0.51284	
	St Lucia-SL8344 ^a	–	5.08	0.69	177	3.3	2.03	0.70	0.70413	0.51296	
	St Vincent-STV301 ^a	–	12.55	0.86	202	5.7	2.47	0.85	0.70382	0.51295	
	St Vincent-STV324 ^a	–	5.12	0.74	236	4.9	2.72	0.94	0.70399	0.51291	
	Grenada-LAG4 ^a	–	17.38	0.89	296	9.3	2.6	2.41	0.70508	0.51284	
	Altered basalt 543 16 5 20-24 ^a	–	–	–	–	–	3.36	–	0.70304	0.51312	
<u>Sediment (increasing depth):</u>											
Site DSDP 543:											
	78A-543-17-3-120-124 ^b	543 18 4W 15-17	174	2.91	–	83	23.5	4.83	8.69	0.714076	0.51207
Site DSDP 144/144A:											
	14-144A-5-1 interval 123-124 ^b	144A 5 1W 119-124	181	0.78	–	750	10.4	1.46	2.31	0.707871	0.51184
	14-144A-6-1 interval 70-110 ^b	144A 6 1W 90-93	190	0.77	–	681	11.5	1.56	2.16	0.707884	0.51183
	14-144Z-4-2 interval 60-64 ^b	144 4 2W 60-64	215	1.21	–	570	6.5	0.97	1.45	0.707806	0.51188
	14-144Z-4-2 interval 143-146 ^b	144 4 2W 60-64	215	1.13	–	570	6.5	0.97	1.45	0.707806	0.51188
	14-144Z-4-3 interval 31-33 ^b	144 4 2W 60-64	215	0.74	–	570	6.5	0.97	1.45	0.707806	0.51188
	14-144Z-4-3 interval 100-103 ^b	144 4 2W 60-64	215	0.85	–	570	6.5	0.97	1.45	0.707806	0.51188
	14-144Z-5-1 interval 5-6 ^b	144 5 1W 123-125	265	0.39	–	446	22.5	4.2	6.39	0.708556	0.51211
	14-144Z-5-1 interval 143-143 ^b	144 5 1W 123-125	265	0.45	–	446	22.5	4.2	6.39	0.708556	0.51211
	14-144Z-7-1 interval 136-137 ^b	144 7 1W 80-82	299	0.28	–	270	28.8	5.4	8.42	0.710830	0.51211
	14-144Z-7-1 interval 123-124 ^b	144 7 1W 80-82	299	0.13	–	270	28.8	5.4	8.42	0.710830	0.51211
	14-144Z-8-3 interval 136-137 ^b	144 8 3W 130-135	328	0.29	–	349	29.4	5.5	8.19	0.710293	0.51210

^a Data from from Van Soest (2000) (LAS1; LAG4), Davidson (1984;1986) (R8204; M8328; Altered basalt), Bezard et al. (2014; under review) (SL8344); Dufrane et al. (2009) (GUAD510) and Heat et al. (1998) (STV301; STV 324).

^b Data indicated correspond to the samples analysed by Carpentier et al. (2008; 2009) named in the table.

Table 3 : AFC model parameters

Endmember compositions^a		
	Initial Magma^b	Assimilant^c
Sr (ppm)	296	790
Os (ppb)	0.36	0.02
La (ppm)	9.32	4.00
Sm (ppm)	2.60	1.84
Th (ppm)	2.41	0.50
⁸⁷ Sr/ ⁸⁶ Sr	0.7051	0.7023
¹⁸⁷ Os/ ¹⁸⁸ Os	0.1268	0.2450

Bulk partition coefficients		
	Model 1	Model 2
DSr	1.4	1.8
DOs	16	12
DTh	2.7	2.3
DLa	2	2.6
DSm	1.3	1.3
$r = Ma/Mc^c$	0.56	0.70

^aused in both models 1 and 2

^b composition of LAG 4 picrite

^c determined iteratively